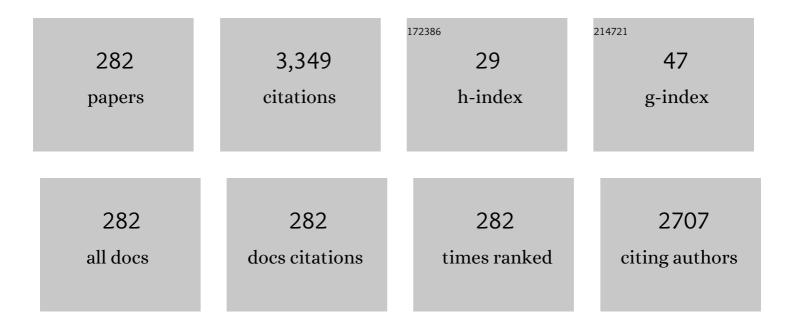
Guoqing Zhou

List of Publications by Year in descending order

Source: https://exaly.com/author-pdf/1578629/publications.pdf Version: 2024-02-01



#	Article	IF	CITATIONS
1	Estimating mangrove above-ground biomass at Maowei Sea, Beibu Gulf of China using machine learning algorithm with Sentinel-1 and Sentinel-2 data. Geocarto International, 2024, 37, 15778-15805.	1.7	7
2	Quantification of Alpine Grassland Fractional Vegetation Cover Retrieval Uncertainty Based on Multiscale Remote Sensing Data. IEEE Geoscience and Remote Sensing Letters, 2022, 19, 1-5.	1.4	1
3	Clumping Effects in Leaf Area Index Retrieval From Large-Footprint Full-Waveform LiDAR. IEEE Transactions on Geoscience and Remote Sensing, 2022, 60, 1-20.	2.7	7
4	Landscape Pattern and Ecological Risk Assessment in Guangxi Based on Land Use Change. International Journal of Environmental Research and Public Health, 2022, 19, 1595.	1.2	33
5	Gaussian Inflection Point Selection for LiDAR Hidden Echo Signal Decomposition. IEEE Geoscience and Remote Sensing Letters, 2022, 19, 1-5.	1.4	40
6	Voids Filling of DEM with Multiattention Generative Adversarial Network Model. Remote Sensing, 2022, 14, 1206.	1.8	30
7	Aboveground biomass of typical invasive mangroves and its distribution patterns using UAV-LiDAR data in a subtropical estuary: Maoling River estuary, Guangxi, China. Ecological Indicators, 2022, 136, 108694.	2.6	23
8	Continuous space ant colony algorithm for automatic selection of orthophoto mosaic seamline network. ISPRS Journal of Photogrammetry and Remote Sensing, 2022, 186, 201-217.	4.9	32
9	Study on Pixel Entanglement Theory for Imagery Classification. IEEE Transactions on Geoscience and Remote Sensing, 2022, 60, 1-18.	2.7	13
10	Identifying spatiotemporal characteristics and driving factors for road traffic CO2 emissions. Science of the Total Environment, 2022, 834, 155270.	3.9	27
11	Spatial Negative Co-Location Pattern Directional Mining Algorithm with Join-Based Prevalence. Remote Sensing, 2022, 14, 2103.	1.8	9
12	Construction of Ecological Security Pattern Based on the Importance of Ecological Protection—A Case Study of Guangxi, a Karst Region in China. International Journal of Environmental Research and Public Health, 2022, 19, 5699.	1.2	18
13	The Development of A Rigorous Model for Bathymetric Mapping from Multispectral Satellite-Images. Remote Sensing, 2022, 14, 2495.	1.8	16
14	Exploring the Potential of UAV LiDAR Data for Trunk Point Extraction and Direct DBH Measurement. Remote Sensing, 2022, 14, 2753.	1.8	9
15	LiDAR Echo Gaussian Decomposition Algorithm for FPGA Implementation. Sensors, 2022, 22, 4628.	2.1	8
16	Single Scanner BLS System for Forest Plot Mapping. IEEE Transactions on Geoscience and Remote Sensing, 2021, 59, 1675-1685.	2.7	14
17	A Multiband Model With Successive Projections Algorithm for Bathymetry Estimation Based on Remotely Sensed Hyperspectral Data in Qinghai Lake. IEEE Journal of Selected Topics in Applied Earth Observations and Remote Sensing, 2021, 14, 6871-6881.	2.3	10
10	Concredized Ruffering Algorithm IEEE Access 2021 9 27140 27157	26	02

18 Generalized Buffering Algorithm. IEEE Access, 2021, 9, 27140-27157.

2.6 93

#	Article	IF	CITATIONS
19	Comparison Analysis of Five Waveform Decomposition Algorithms for the Airborne LiDAR Echo Signal. IEEE Journal of Selected Topics in Applied Earth Observations and Remote Sensing, 2021, 14, 7869-7880.	2.3	50
20	Chaotic Macropulse Green Laser Beam Generated by Modulating a 520 nm Laser Diode with Optical Feedback. Journal of Russian Laser Research, 2021, 42, 66-74.	0.3	1
21	Footprint Size Design of Large-Footprint Full-Waveform LiDAR for Forest and Topography Applications: A Theoretical Study. IEEE Transactions on Geoscience and Remote Sensing, 2021, 59, 9745-9757.	2.7	10
22	MODIS-Based Research on Secchi Disk Depth Using an Improved Semianalytical Algorithm in the Yellow Sea. IEEE Journal of Selected Topics in Applied Earth Observations and Remote Sensing, 2021, 14, 5964-5972.	2.3	4
23	Design of supercontinuum laser hyperspectral light detection and ranging (LiDAR) (SCLaHS LiDAR). International Journal of Remote Sensing, 2021, 42, 3731-3755.	1.3	71
24	Selection of Optimal Building Facade Texture Images From UAV-Based Multiple Oblique Image Flows. IEEE Transactions on Geoscience and Remote Sensing, 2021, 59, 1534-1552.	2.7	56
25	Automated Marker-Free Registration of Multisource Forest Point Clouds Using a Coarse-to-Global Adjustment Strategy. Forests, 2021, 12, 269.	0.9	10
26	Maximal Instance Algorithm for Fast Mining of Spatial Co-Location Patterns. Remote Sensing, 2021, 13, 960.	1.8	4
27	Maize and soybean heights estimation from unmanned aerial vehicle (UAV) LiDAR data. Computers and Electronics in Agriculture, 2021, 182, 106005.	3.7	39
28	A Novel Strategy to Reconstruct NDVI Time-Series with High Temporal Resolution from MODIS Multi-Temporal Composite Products. Remote Sensing, 2021, 13, 1397.	1.8	11
29	Quantitative Evaluation of Leaf Inclination Angle Distribution on Leaf Area Index Retrieval of Coniferous Canopies. Journal of Remote Sensing, 2021, 2021, .	3.2	14
30	Collection Method of Arbitrary Laser Echo Based on STM32. IOP Conference Series: Earth and Environmental Science, 2021, 783, 012146.	0.2	0
31	Underwater Signal Measurement and Transmission Experiment Equipment Design for LIDAR. IOP Conference Series: Earth and Environmental Science, 2021, 783, 012086.	0.2	0
32	Study on Local to Global Radiometric Balance for Remotely Sensed Imagery. Remote Sensing, 2021, 13, 2068.	1.8	5
33	Fisheye Image Correction Based on Three-Dimensional Control Field. IOP Conference Series: Earth and Environmental Science, 2021, 783, 012073.	0.2	1
34	Orientation of Small UAV Images with Constraint. IOP Conference Series: Earth and Environmental Science, 2021, 783, 012094.	0.2	0
35	8-Day and Daily Maximum and Minimum Air Temperature Estimation via Machine Learning Method on a Climate Zone to Global Scale. Remote Sensing, 2021, 13, 2355.	1.8	7
36	Seed point set-based building roof extraction from airborne LiDAR point clouds using a top-down strategy. Automation in Construction, 2021, 126, 103660.	4.8	28

#	Article	IF	CITATIONS
37	Non-Uniformity Correction of Infrared Images Based on Improved CNN With Long-Short Connections. IEEE Photonics Journal, 2021, 13, 1-13.	1.0	3
38	An Incremental Isomap Method for Hyperspectral Dimensionality Reduction and Classification. Photogrammetric Engineering and Remote Sensing, 2021, 87, 445-455.	0.3	0
39	Aboveground mangrove biomass estimation in Beibu Gulf using machine learning and UAV remote sensing. Science of the Total Environment, 2021, 781, 146816.	3.9	60
40	Optimal Regularization Method Based on the L-Curve for Solving Rational Function Model Parameters. Photogrammetric Engineering and Remote Sensing, 2021, 87, 661-668.	0.3	3
41	Point cloud denoising using non-local collaborative projections. Pattern Recognition, 2021, 120, 108128.	5.1	12
42	Overview of Underwater Transmission Characteristics of Oceanic LiDAR. IEEE Journal of Selected Topics in Applied Earth Observations and Remote Sensing, 2021, 14, 8144-8159.	2.3	68
43	Landslide Risk Classification Based on Ensemble Machine Learning. , 2021, , .		2
44	Classification of Surface Natural Resources Based on HR-Net and DEM. , 2021, , .		2
45	Improved Gauss Inflection Point Matching Method for Lidar Echo Signal Decomposition. , 2021, , .		0
46	The Reprocessing for Himawari-8 Based on Deep Learning. , 2021, , .		1
47	Fisheye Camera Calibration with Indoor 3D Calibration Field. , 2021, , .		0
48	S-MobileNetV2+SegNet Model and Rapid Identification of Sugarcane. , 2021, , .		0
49	Optimization of Aerial Image Exposure Center with Baseline Constraint Condition Model. , 2021, , .		0
50	Comparative Analysis of the Semi-Empirical Physical Models for Shallow Water Depth Inversion in Beibu Gulf. , 2021, , .		0
51	Deformation of Chengdu Downtown with Sentinel-1A. , 2021, , .		Ο
52	Evaluation of county-level poverty alleviation progress by deep learning and satellite observations. Big Earth Data, 2021, 5, 576-592.	2.0	5
53	Retrieving building height in urban areas using ICESat-2 photon-counting LiDAR data. International Journal of Applied Earth Observation and Geoinformation, 2021, 104, 102596.	1.4	11
54	An innovative echo detection system with STM32 gated and PMT adjustable gain for airborne LiDAR. International Journal of Remote Sensing, 2021, 42, 9187-9211.	1.3	86

#	Article	IF	CITATIONS
55	Correcting Crown-Level Clumping Effect for Improving Leaf Area Index Retrieval From Large-Footprint LiDAR: A Study Based on the Simulated Waveform and GLAS Data. IEEE Journal of Selected Topics in Applied Earth Observations and Remote Sensing, 2021, 14, 12386-12402.	2.3	4
56	Impacts of Urban land surface temperature on tract landscape pattern, physical and social variables. International Journal of Remote Sensing, 2020, 41, 683-703.	1.3	20
57	Zero-Doppler Centroid Steering for the Moon-Based Synthetic Aperture Radar: A Theoretical Analysis. IEEE Geoscience and Remote Sensing Letters, 2020, 17, 1208-1212.	1.4	13
58	Study of an SCSC-OSM for the Creation of an Urban Three-Dimensional Building. IEEE Access, 2020, 8, 126266-126283.	2.6	2
59	Estimation of karst carbon sink and its contribution to CO2 emissions over a decade using remote sensing imagery. Applied Geochemistry, 2020, 121, 104689.	1.4	8
60	Patch Pattern and Ecological Risk Assessment of Alpine Grassland in the Source Region of the Yellow River. Remote Sensing, 2020, 12, 3460.	1.8	13
61	Ground Control Point Automatic Extraction for Spaceborne Georeferencing Based on FPGA. IEEE Journal of Selected Topics in Applied Earth Observations and Remote Sensing, 2020, 13, 3350-3366.	2.3	4
62	Building Shadow Detection on Ghost Images. Remote Sensing, 2020, 12, 679.	1.8	11
63	Reconstructing facade semantic models using hierarchical topological graphs. Transactions in GIS, 2020, 24, 1073-1097.	1.0	6
64	Warning of Rainfall-Induced Landslide in Bazhou District. , 2020, , .		3
65	Scattering Mechanism of Large-Footprint Full-Waveform Lidar Over Mountainous Forest Areas. , 2020, , .		0
66	Drought Monitoring in Sub-Sahara Africa. , 2020, , .		0
67	Change of Glacial Lake in Karakoram Range. , 2020, , .		1
68	Design of LiDAR optical-mechanical system for water depth measurement. Hongwai Yu Jiguang Gongcheng/Infrared and Laser Engineering, 2020, 49, 203006.	0.1	1
69	Inference of Urban Function Zone Based on Deep Neural Network. , 2020, , .		1
70	Ship Detection with Sar Based on Yolo. , 2020, , .		10
71	Land Use and Land Cover Change of Ghana. , 2020, , .		0
72	DEM correction to the TVDI method on drought monitoring in karst areas. International Journal of Remote Sensing, 2019, 40, 2166-2189.	1.3	23

#	Article	IF	CITATIONS
73	Real-time ortho-rectification for remote-sensing images. International Journal of Remote Sensing, 2019, 40, 2451-2465.	1.3	8
74	Estimating forest aboveground biomass using small-footprint full-waveform airborne LiDAR data. International Journal of Applied Earth Observation and Geoinformation, 2019, 83, 101922.	1.4	14
75	Assessing the Impact of the Built-Up Environment on Nighttime Lights in China. Remote Sensing, 2019, 11, 1712.	1.8	8
76	Multiscale SAR image segmentation by combining curvelet transform and GMTRJ algorithms. , 2019, 95, 102583.		3
77	An Energy-Based SAR Image Segmentation Method with Weighted Feature. Remote Sensing, 2019, 11, 1169.	1.8	7
78	Combining hyperspectral imagery and LiDAR pseudo-waveform for predicting crop LAI, canopy height and above-ground biomass. Ecological Indicators, 2019, 102, 801-812.	2.6	31
79	Structural Optimization of Receiving System Based on Optimal Field of View for Shallow Sea Laser Measurement. , 2019, , .		0
80	Classification Based on Capsule Network with Hyperspectral Image. , 2019, , .		4
81	On-Board Wavelet Based Change Detection Implementation of SAR Flood Image. , 2019, , .		1
82	Effects of the Earth's Irregular Rotation on the Moon-Based Synthetic Aperture Radar Imaging. IEEE Access, 2019, 7, 155014-155027.	2.6	8
83	Urban Functional Regions Discovering Based on Deep Learning. , 2019, , .		1
84	Land Price Assesment Based on Deep Neural Network. , 2019, , .		0
85	Building Shadow Determination Based on Dbm. , 2019, , .		1
86	On-Board Georeferencing Using FPGA-Based Optimized Second-Order Polynomial Equation. Remote Sensing, 2019, 11, 124.	1.8	11
87	Spatiotemporal distribution of net primary productivity and its driving factors in the Nanliu River basin in the Beibu Gulf. Acta Ecologica Sinica, 2019, 39, .	0.0	4
88	Lithologic classification using multilevel spectral characteristics. Journal of Applied Remote Sensing, 2019, 13, 1.	0.6	6
89	A Manifold Learning Approach of Land Cover Classification for Optical and SAR Fusing Data. , 2018, , .		1

90 Urban Functional Regions Using Social Media Check-Ins. , 2018, , .

#	Article	IF	CITATIONS
91	An Improved Adaptive Ant Colony Algorithm for Intelligent Seamline Detection of Orthoimage Mosaicking. , 2018, , .		1
92	FPGA-Based On-Board Geometric Calibration for Linear CCD Array Sensors. Sensors, 2018, 18, 1794.	2.1	7
93	RPC-Based Orthorectification for Satellite Images Using FPGA. Sensors, 2018, 18, 2511.	2.1	8
94	Integration of Airborne LiDAR and Hyperspectral Data for Maize FPAR Estimation Based on a Physical Model. IEEE Geoscience and Remote Sensing Letters, 2018, 15, 1120-1124.	1.4	7
95	Projection learning with local and global consistency constraints for scene classification. ISPRS Journal of Photogrammetry and Remote Sensing, 2018, 144, 202-216.	4.9	9
96	Hierarchical spatial features learning with deep CNNs for very high-resolution remote sensing image classification. International Journal of Remote Sensing, 2018, 39, 5978-5996.	1.3	9
97	A New FPGA Architecture of FAST and BRIEF Algorithm for On-Board Corner Detection and Matching. Sensors, 2018, 18, 1014.	2.1	25
98	An FPGA-based implementation of corner detection and matching with outlier rejection. International Journal of Remote Sensing, 2018, 39, 8905-8933.	1.3	4
99	Saturated Echo Signal Algorithm for Wide Dynamic Range Lidar. Guangzi Xuebao/Acta Photonica Sinica, 2018, 47, 1228003.	0.1	Ο
100	Multi-channel Processing Technology for Wide Dynamic Range Signal in Airborne Lidar Bathymetry. Guangzi Xuebao/Acta Photonica Sinica, 2018, 47, 301002.	0.1	0
101	Building Occlusion Detection From Ghost Images. IEEE Transactions on Geoscience and Remote Sensing, 2017, 55, 1074-1084.	2.7	18
102	A new approach to minimize walk error in pulsed laser rangefinding. , 2017, , .		2
103	Onboard ortho-rectification for remotely sensed images. , 2017, , .		1
104	On-board detection and matching of remotely sensing imagery. , 2017, , .		1
105	Carbon sink estimation of surface carbonate karstification in global karst area. , 2017, , .		1
106	Design of a CMOS ROIC for InGaAs Self-Mixing Detectors Used in FM/cw LADAR. IEEE Sensors Journal, 2017, 17, 5547-5557.	2.4	10
107	Estimation of coniferous forest aboveground biomass with aggregated airborne small-footprint LiDAR full-waveforms. Optics Express, 2017, 25, A851.	1.7	13
108	On-Board Detection and Matching of Feature Points. Remote Sensing, 2017, 9, 601.	1.8	15

#	Article	IF	CITATIONS
109	Monitoring of Subsidence along Jingjin Inter-City Railway with High-Resolution TerraSAR-X MT-InSAR Analysis. Remote Sensing, 2017, 9, 717.	1.8	25
110	On-Board Ortho-Rectification for Images Based on an FPGA. Remote Sensing, 2017, 9, 874.	1.8	20
111	Simulating the Effects of the Airborne Lidar Scanning Angle, Flying Altitude, and Pulse Density for Forest Foliage Profile Retrieval. Applied Sciences (Switzerland), 2017, 7, 712.	1.3	18
112	Spatial-Temporal Analysis of Carbonate Outcrop in South America with Response of Global CO2 Sink. , 2017, , .		1
113	Maximum variance unfolding based co-location decision tree for remote sensing image classification. , 2017, , .		2
114	FPGA-Based N×N adaptive channel for array lidar imager. , 2017, , .		1
115	97-μJ single frequency linearly polarized nanosecond pulsed laser at 775Ânm using frequency doubling of a high-energy fiber laser system. Optical Engineering, 2017, 56, 1.	0.5	3
116	High precision pixel readout circuit design for GM-APD array. Hongwai Yu Jiguang Gongcheng/Infrared and Laser Engineering, 2017, 46, 106007.	0.1	1
117	Absolute Orientation Based on Distance Kernel Functions. Remote Sensing, 2016, 8, 213.	1.8	4
118	Transformation Model with Constraints for High-Accuracy of 2D-3D Building Registration in Aerial Imagery. Remote Sensing, 2016, 8, 507.	1.8	5
119	Second-Order Polynomial Equation-Based Block Adjustment for Orthorectification of DISP Imagery. Remote Sensing, 2016, 8, 680.	1.8	8
120	Manifold Learning Co-Location Decision Tree for Remotely Sensed Imagery Classification. Remote Sensing, 2016, 8, 855.	1.8	13
121	Estimation of Soil Moisture from Optical and Thermal Remote Sensing: A Review. Sensors, 2016, 16, 1308.	2.1	175
122	Occlusion detection for urban aerial true orthoimage generation. , 2016, , .		4
123	Uncertainties analysis for normalized soil moisture model based on the combination of optical and thermal infrared data. , 2016, , .		1
124	Automatically texture extraction, mapping and 3D visualizaiton of buildings facades based on high resolution aerial photos. , 2016, , .		0
125	A new method of occlusion detection to generate true orthophoto. , 2016, , .		0
126	Revealing the early ice flow patterns with historical Declassified Intelligence Satellite Photographs back to 1960s. Geophysical Research Letters, 2016, 43, 5758-5767.	1.5	18

#	Article	IF	CITATIONS
127	Spatial analysis for susceptibility of second-time karst sinkholes: A case study of Jili Village in Guangxi, China. Computers and Geosciences, 2016, 89, 144-160.	2.0	25
128	Texture mapping based on multiple aerial imageries in urban areas. , 2015, , .		1
129	Inversion of ocean wave spectra from SAR imagery in Beibu Gulf. , 2015, , .		0
130	Drought monitoring and warning in the middle reach of Yangtze River with MODIS. , 2015, , .		0
131	Estimation and Validation of Land Surface Temperatures from Chinese Second-Generation Polar-Orbit FY-3A VIRR Data. Remote Sensing, 2015, 7, 3250-3273.	1.8	55
132	Sea Surface Wind Retrievals from SIR-C/X-SAR Data: A Revisit. Remote Sensing, 2015, 7, 3548-3564.	1.8	10
133	A Multi-Channel Method for Retrieving Surface Temperature for High-Emissivity Surfaces from Hyperspectral Thermal Infrared Images. Sensors, 2015, 15, 13406-13423.	2.1	7
134	Adaptive graph construction for Isomap manifold learning. Proceedings of SPIE, 2015, , .	0.8	2
135	Comparison and analysis of soil moisture retrieval model from CBERS-02B satellite imagery. , 2015, , .		2
136	The application of ant colony algorithm in emergency rescue with GIS. , 2015, , .		0
137	INSAR railway monitoring validation through high density leveling campaign. , 2015, , .		1
138	Based on Landsat8 multi-resolution remote sensing image fusion of urban heat-island difference analysis. , 2015, , .		0
139	FPGA-based remotely sensed imagery denoising. , 2015, , .		0
140	Advances and perspectives of on-orbit geometric calibration for high-resolution optical satellites. , 2015, , .		0
141	Change analysis of karst rocky desertification for almost 40 years: a case study of Guangxi, China. Proceedings of SPIE, 2015, , .	0.8	0
142	Comparative analysis of surface soil moisture retrieval using VSWI and TVDI in karst areas. , 2015, , .		2
143	Building facade texture extracted from high-resolution aerial photo. Proceedings of SPIE, 2015, , .	0.8	0

Advances and perspectives in bathymetry by airborne lidar. , 2015, , .

#	Article	IF	CITATIONS
145	FPCA-based data processing module design of on-board radiometric calibration in visible/near infrared bands. , 2015, , .		0
146	Effects of vegetation types on soil moisture estimation from the normalized land surface temperature versus vegetation index space. , 2015, , .		0
147	The texture extraction and mapping of buildings with occlusion detection. , 2015, , .		5
148	3D image generation with laser radar based on APD arrays. , 2015, , .		2
149	Sparse coding based dense feature representation model for hyperspectral image classification. Journal of Electronic Imaging, 2015, 24, 063009.	0.5	7
150	An integrated approach for shadow detection of the building in urban areas. , 2015, , .		1
151	Extension of the Generalized Split-Window Algorithm for Land Surface Temperature Retrieval to Atmospheres With Heavy Dust Aerosol Loading. IEEE Journal of Selected Topics in Applied Earth Observations and Remote Sensing, 2015, 8, 825-834.	2.3	9
152	Overview of 30years of research on solubility trapping in Chinese karst. Earth-Science Reviews, 2015, 146, 183-194.	4.0	28
153	Flash Lidar Sensor Using Fiber-Coupled APDs. IEEE Sensors Journal, 2015, 15, 4758-4768.	2.4	40
154	Evaluation of the wave energy conditions along the coastal waters ofÂBeibu Gulf, China. Energy, 2015, 85, 449-457.	4.5	21
155	Multiscale Validation of the 8-day MOD16 Evapotranspiration Product Using Flux Data Collected in China. IEEE Journal of Selected Topics in Applied Earth Observations and Remote Sensing, 2015, 8, 1478-1486.	2.3	56
156	Research of Job Scheduling With Cloud Based On Trust Mechanism And SFLA. International Journal of Grid and Distributed Computing, 2015, 8, 93-100.	0.8	3
157	Assessment of two temporal-information-based methods for estimating evaporative fraction over the Southern Great Plains. International Journal of Remote Sensing, 2015, 36, 4936-4952.	1.3	8
158	A New Model for Surface Soil Moisture Retrieval From CBERS-02B Satellite Imagery. IEEE Journal of Selected Topics in Applied Earth Observations and Remote Sensing, 2015, 8, 628-637.	2.3	6
159	Temporal-spatial distribution of wave energy: A case study of Beibu Gulf, China. Renewable Energy, 2015, 74, 344-356.	4.3	30
160	Daily Evaporative Fraction Parameterization Scheme Driven by Day–Night Differences in Surface Parameters: Improvement and Validation. Remote Sensing, 2014, 6, 4369-4390.	1.8	8
161	Establishment of rocky desertification index in Southwest of China. , 2014, , .		0
162	Co-location decision tree model for extracting exposed carbonate rocks in karst rocky desertification area. , 2014, , .		1

Guoqing Zhou

#	Article	IF	Citations
163	Risk evaluation of Karst collapse using GIS and RS. , 2014, , .		Ο
164	Extraction of exposed carbonatite in karst desertification area using co-location decision tree. , 2014, , .		1
165	The ecological environment assessment and repairing of Guilin Karst Scenery based on satellite remote sensing. , 2014, , .		2
166	3D flash lidar imager onboard UAV. , 2014, , .		0
167	Data analysis of karst collapse based on GIS: A case study of Jili, Guangxi. , 2014, , .		Ο
168	Seamless Fusion of LiDAR and Aerial Imagery for Building Extraction. IEEE Transactions on Geoscience and Remote Sensing, 2014, 52, 7393-7407.	2.7	71
169	Estimation of Diurnal Cycle of Land Surface Temperature at High Temporal and Spatial Resolution from Clear-Sky MODIS Data. Remote Sensing, 2014, 6, 3247-3262.	1.8	71
170	On massive spatial data cloud storage and quad-tree index based on the HBase. , 2014, , .		2
171	Evaluating the SEBSâ€estimated evaporative fraction from MODIS data for a complex underlying surface. Hydrological Processes, 2013, 27, 3139-3149.	1.1	13
172	Determination of bare surface soil moisture from combined temporal evolution of land surface temperature and net surface shortwave radiation. Hydrological Processes, 2013, 27, 2825-2833.	1.1	25
173	Hyperspectral image classification using a spectral-spatial sparse coding model. Proceedings of SPIE, 2013, , .	0.8	3
174	Retrieval of wave parameters from ERS-2 SAR imagery in shallow ocean area. , 2013, , .		0
175	Effect of Basalt Fiber on the Asphalt Binder and Mastic at Low Temperature. Journal of Materials in Civil Engineering, 2013, 25, 355-364.	1.3	65
176	Modeling of Day-to-Day Temporal Progression of Clear-Sky Land Surface Temperature. IEEE Geoscience and Remote Sensing Letters, 2013, 10, 1050-1054.	1.4	32
177	A Novel Vehicle Detection Method With High Resolution Highway Aerial Image. IEEE Journal of Selected Topics in Applied Earth Observations and Remote Sensing, 2013, 6, 2338-2343.	2.3	62
178	Simulation study of new generation of airborne scannerless LiDAR system. , 2013, , .		1
179	Generation of pixel-level resolution lunar DEM based on Chang'E-1 three-line imagery and laser altimeter data. Computers and Geosciences, 2013, 59, 53-59.	2.0	2
180	A novel building boundary reconstruction method based on lidar data and images. , 2013, , .		4

A novel building boundary reconstruction method based on lidar data and images. , 2013, , . 180

#	Article	IF	CITATIONS
181	The relation between accuracy and size of structure element for vehicle detection with high resolution highway aerial images. , 2013, , .		4
182	Fatigue Properties of Asphalt Materials at Low In-Service Temperatures. Journal of Materials in Civil Engineering, 2013, 25, 1220-1227.	1.3	18
183	Using GPS buoy to verify SWH and AP of SAR inversion. , 2013, , .		Ο
184	Retrieval of ocean wavelength and wave direction from SAR image based on radon transform. , 2013, , .		5
185	A new model for surface soil moisture retrieval from CBERS-02B satellite imagery in karst area. , 2013, ,		Ο
186	Simulation study on SAR imaging spectrum of shallow water area using Texel-Marsen-Arsloe spectrum. , 2013, , .		0
187	Extracting corn geometric structural parameters using Kinect. , 2012, , .		2
188	Comparison of object-oriented and Maximum Likelihood Classification of land use in Karst area. , 2012,		3
189	Analysis of land use and cover change in Sichuan province, China. Journal of Applied Remote Sensing, 2012, 6, 063587.	0.6	7
190	Rocky desertification exponential model in Karst area. , 2012, , .		0
191	Research on non-linear fusion deformation analysis and forecast method. , 2012, , .		Ο
192	Evaluating the severity level of cotton <i>Verticillium</i> using spectral signature analysis. International Journal of Remote Sensing, 2012, 33, 2706-2724.	1.3	43
193	Vehicle detection based on morphology from highway aerial images. , 2012, , .		19
194	Fatigue of asphalt binder, mastic and mixture at low temperature. Frontiers of Structural and Civil Engineering, 2012, 6, 166-175.	1.2	8
195	Co-location decision tree for enhancing decision-making of pavement maintenance and rehabilitation. Transportation Research Part C: Emerging Technologies, 2012, 21, 287-305.	3.9	35
196	Power supply topology for lidar system onboard UAV platform. , 2011, , .		3
197	Effect of Permeameter Size and Anisotropy on Measurements of Field Pavement Permeability. Transportation Research Record, 2011, 2209, 41-51.	1.0	4
198	Design and Implementation of Power Supply of High-Power Diode Laser of LiDAR Onboard UAV. , 2011, , .		3

#	Article	IF	CITATIONS
199	UAV-based multi-sensor data fusion processing. International Journal of Image and Data Fusion, 2010, 1, 283-291.	0.8	7
200	Integration of GIS and Data Mining Technology to Enhance the Pavement Management Decision Making. Journal of Transportation Engineering, 2010, 136, 332-341.	0.9	46
201	Geo-Referencing of Video Flow From Small Low-Cost Civilian UAV. IEEE Transactions on Automation Science and Engineering, 2010, 7, 156-166.	3.4	19
202	Extracting trees and structure parameters via integration of LIDAR data and ground imagery. , 2010, , .		0
203	Image-based 3D corn reconstruction for retrieval of geometrical structural parameters. International Journal of Remote Sensing, 2009, 30, 5505-5513.	1.3	25
204	Coastal 3-D Morphological Change Analysis Using LiDAR Series Data: A Case Study of Assateague Island National Seashore. Journal of Coastal Research, 2009, 252, 435-447.	0.1	43
205	Near Real-Time Orthorectification and Mosaic of Small UAV Video Flow for Time-Critical Event Response. IEEE Transactions on Geoscience and Remote Sensing, 2009, 47, 739-747.	2.7	75
206	Foreword to the Special Issue on Unmanned Airborne Vehicle (UAV) Sensing Systems for Earth Observations. IEEE Transactions on Geoscience and Remote Sensing, 2009, 47, 687-689.	2.7	43
207	High-accuracy of orthorectification model with self-geometric constraint for high buildings in urban area. , 2009, , .		0
208	Accurate pose and location estimation of uncalibrated camera in urban area. , 2009, , .		2
209	A Bayesian network algorithm for retrieving the characterization of land surface vegetation. Remote Sensing of Environment, 2008, 112, 613-622.	4.6	48
210	Orthoimage Creation of Extremely High Buildings. IEEE Transactions on Geoscience and Remote Sensing, 2008, 46, 4132-4141.	2.7	10
211	Analysis of Flexible Pavement Distresses on IRI Model. , 2008, , .		4
212	Traffic Spatial Measures and Interpretation of Road Network Using Aerial Remotely Sensed Data. , 2008, , .		0
213	Real-Time UAV Ortho Video Generation. , 2008, , .		1
214	Survey and Analysis of Land Satellite Remote Sensing Applied in Highway Transportations Infrastructure and System Engineering. , 2008, , .		2
215	Study on blimp-based low-cost remote sensing platform. , 2008, , .		0
216	Road network spatial data co-registration of different sources using imagery-to-GIS mining. , 2007, , .		0

#	Article	IF	CITATIONS
217	Area spatial object co-registration between imagery and GIS data for spatial-temporal change analysis. , 2007, , .		1
218	Geo-registration and mosaic of UAV video for quick-response to forest fire disaster. , 2007, 6788, 259.		5
219	Space-Ground Sensor Web for Study of Urban Micro-Environment. , 2007, , .		0
220	Civil UAV system for earth observation. , 2007, , .		17
221	Automatic Extraction of Power Lines From Aerial Images. IEEE Geoscience and Remote Sensing Letters, 2007, 4, 387-391.	1.4	140
222	POS supported sparse bundle adjustment and its application in power line inspection. , 2006, , .		0
223	True Orthoimage Generation for Urban Areas with Very High Buildings. , 2006, , 1-18.		0
224	Accuracy improvement of urban true orthoimage generation using 3D R-tree-based urban model. , 2006, , ,		5
225	National large-scale Urban True Orthophoto Mapping and its standard initiative. , 2006, , .		0
226	Customizing Visualization in Three-Dimensional Urban GIS via Web-Based Interaction. Journal of the Urban Planning and Development Division, ASCE, 2006, 132, 97-103.	0.8	27
227	A new method for debris flow detection using multiâ€ŧemporal DEMs without ground control points. International Journal of Remote Sensing, 2006, 27, 4911-4921.	1.3	9
228	A comprehensive study on urban true orthorectification. IEEE Transactions on Geoscience and Remote Sensing, 2005, 43, 2138-2147.	2.7	89
229	Urban surface model generation from remotely sensed airborne image sequence data. International Journal of Remote Sensing, 2005, 26, 79-98.	1.3	5
230	True orthoimage generation in urban areas with very tall buildings. International Journal of Remote Sensing, 2004, 25, 5163-5180.	1.3	26
231	Urban 3D GIS From LiDAR and digital aerial images. Computers and Geosciences, 2004, 30, 345-353.	2.0	101
232	Satellite Navigation Parameter-Assisted Orthorectification for over 60°N Latitude Satellite Imagery. Photogrammetric Engineering and Remote Sensing, 2004, 70, 1021-1029.	0.3	0
233	Post-launch geometric calibration of linear array imaging system. , 2003, , .		0
234	Future intelligent Earth observing satellites. , 2003, 5151, 1.		9

Guoqing Zhou

#	Article	IF	CITATIONS
235	Satellite photograph mosaics of Greenland from the 1960s era. International Journal of Remote Sensing, 2002, 23, 1143-1159.	1.3	26
236	Orthorectification of 1960s satellite photographs covering Greenland. IEEE Transactions on Geoscience and Remote Sensing, 2002, 40, 1247-1259.	2.7	23
237	Design and Implementation of Attribute Database Management System in A GIS System: GeoStar. Annals of GIS, 2000, 6, 170-180.	1.4	3
238	CCD CAMERA CALIBRATION BASED ON NATURAL LANDMARKS. Pattern Recognition, 1998, 31, 1715-1724.	5.1	12
239	Primitive recognition using aspect-interpretation model matching in both CAD- and LP-based measurement systems. ISPRS Journal of Photogrammetry and Remote Sensing, 1997, 52, 74-84.	4.9	0
240	Future earth observing satellites. , 0, , .		0
241	US National Large-scale City orthoimage standard initiative. , 0, , .		0
242	Comparison of satellite measured temperatures using terra ASTER and landsat ETM+ data. , 0, , .		3
243	Future Earth observation strategy for societal benefits. , 0, , .		1
244	Urban large-scale orthoimage standard for national orthophoto program. , 0, , .		4
245	AN IMPROVED METHOD OF AGM FOR HIGH PRECISION GEOLOCATION OF SAR IMAGES. International Archives of the Photogrammetry, Remote Sensing and Spatial Information Sciences - ISPRS Archives, 0, XLII-3, 2479-2485.	0.2	3
246	A BUFFER ANALYSIS BASED ON CO-LOCATION ALGORITHM. International Archives of the Photogrammetry, Remote Sensing and Spatial Information Sciences - ISPRS Archives, 0, XLII-3, 2487-2490.	0.2	3
247	MINING CO-LOCATION PATTERNS WITH CLUSTERING ITEMS FROM SPATIAL DATA SETS. International Archives of the Photogrammetry, Remote Sensing and Spatial Information Sciences - ISPRS Archives, 0, XLII-3, 2505-2509.	0.2	3
248	A NEW GRADUATION ALGORITHM FOR COLOR BALANCE OF REMOTE SENSING IMAGE. International Archives of the Photogrammetry, Remote Sensing and Spatial Information Sciences - ISPRS Archives, 0, XLII-3, 2517-2521.	0.2	3
249	ESTIMATION OF OPTICAL PROPERTIES USING QAA-V6 MODEL BASED ON MODIS DATA. International Archives of the Photogrammetry, Remote Sensing and Spatial Information Sciences - ISPRS Archives, 0, XLII-3/W10, 937-940.	0.2	2
250	An overview of in-orbit radiometric calibration of typical satellite sensors. International Archives of the Photogrammetry, Remote Sensing and Spatial Information Sciences - ISPRS Archives, 0, XL-7/W4, 235-240.	0.2	4
251	AN OPTIONAL THRESHOLD WITH SVM CLOUD DETECTION ALGORITHM AND DSP IMPLEMENTATION. International Archives of the Photogrammetry, Remote Sensing and Spatial Information Sciences - ISPRS Archives, 0, XLI-B8, 771-777.	0.2	4
252	Future Intelligent Earth Observing Satellite System (FIEOS): Advanced System of Systems. , 0, , .		5

Future Intelligent Earth Observing Satellite System (FIEOS): Advanced System of Systems. , 0, , . 252

#	Article	IF	CITATIONS
253	EXTRACTION OF ROCKY DESERTIFICATION FROM DISP IMAGERY: A CASE STUDY OF LIUPANSHUI, GUIZHOU, CHINA. International Archives of the Photogrammetry, Remote Sensing and Spatial Information Sciences - ISPRS Archives, 0, XLII-2/W7, 1061-1065.	0.2	0
254	ESTIMATION OF CARBON SINK IN SURFACE CARBONATE ROCKS OF GUANGXI PROVINCE BY USING REMOTE SENSING IMAGES. International Archives of the Photogrammetry, Remote Sensing and Spatial Information Sciences - ISPRS Archives, 0, XLII-3, 625-628.	0.2	0
255	A NEW APPROACH FOR ACCURACY IMPROVEMENT OF PULSED LIDAR REMOTE SENSING DATA. International Archives of the Photogrammetry, Remote Sensing and Spatial Information Sciences - ISPRS Archives, 0, XLII-3, 2491-2494.	0.2	1
256	IMPROVEMENT ON TIMING ACCURACY OF LIDAR FOR REMOTE SENSING. International Archives of the Photogrammetry, Remote Sensing and Spatial Information Sciences - ISPRS Archives, 0, XLII-3, 2495-2498.	0.2	0
257	HYBRID MODELING BASED ON SCSG-BR AND ORTHOPHOTO. International Archives of the Photogrammetry, Remote Sensing and Spatial Information Sciences - ISPRS Archives, 0, XLII-3, 2499-2503.	0.2	1
258	SOLVING THE RATIONAL POLYNOMIAL COEFFICIENTS BASED ON L CURVE. International Archives of the Photogrammetry, Remote Sensing and Spatial Information Sciences - ISPRS Archives, 0, XLII-3, 2511-2515.	0.2	1
259	AN ISOMETRIC MAPPING BASED CO-LOCATION DECISION TREE ALGORITHM. International Archives of the Photogrammetry, Remote Sensing and Spatial Information Sciences - ISPRS Archives, 0, XLII-3, 2531-2534.	0.2	0
260	VECTOR AND RASTER DATA LAYERED FUSION AND 3D VISUALIZATION. International Archives of the Photogrammetry, Remote Sensing and Spatial Information Sciences - ISPRS Archives, 0, XLII-3/W10, 1127-1134.	0.2	0
261	HPR AND OPK ANGLE ELEMENT CONVERSION METHOD BASED ON AIRBORNE LIDAR ALIGNMENT AXIS ERROR CALIBRATION. International Archives of the Photogrammetry, Remote Sensing and Spatial Information Sciences - ISPRS Archives, 0, XLII-3/W10, 71-75.	0.2	1
262	MULTISPECTRAL REMOTE SENSING IMAGE CLASSIFICATION BASED ON QUANTUM ENTANGLEMENT. International Archives of the Photogrammetry, Remote Sensing and Spatial Information Sciences - ISPRS Archives, 0, XLII-3/W10, 667-670.	0.2	0
263	SHALLOW BATHYMETRY ESTIMATION BASED ON LANDSAT 8 REMOTELY SENSED DATAAT BOHAI SEA. International Archives of the Photogrammetry, Remote Sensing and Spatial Information Sciences - ISPRS Archives, 0, XLII-3/W10, 941-943.	0.2	0
264	A PRELIMINARY STUDY ON CLASSIFICATION STANDARDS OF NATURAL RESOURCES UNDER THE INSTITUTIONAL REFORM. International Archives of the Photogrammetry, Remote Sensing and Spatial Information Sciences - ISPRS Archives, 0, XLII-3/W10, 521-524.	0.2	0
265	RESEARCH ON EVALUATION METHOD OF AIRBORNE LIDAR POSITIONING ACCURACY. International Archives of the Photogrammetry, Remote Sensing and Spatial Information Sciences - ISPRS Archives, 0, XLII-3/W10, 825-830.	0.2	0
266	Urban High-Resolution Remote Sensing. , 0, , .		18
267	LIDAR BATHYMETRIC EVALUATION BASED ON SCATTERING CLASSIFICATION ALGORITHM. International Archives of the Photogrammetry, Remote Sensing and Spatial Information Sciences - ISPRS Archives, 0, XLII-3/W10, 97-103.	0.2	0
268	DESIGN OF THREE-CHANNEL OPTICAL RECEIVING SYSTEM FOR DUAL-FREQUENCY LASER RADAR. International Archives of the Photogrammetry, Remote Sensing and Spatial Information Sciences - ISPRS Archives, 0, XLII-3/W10, 815-819.	0.2	2
269	KARST ROCKY DESERTIFICATION ANALYSIS BASED ON HISTORICAL DISP DATA TAKE TWO REGIONS FOR EXAMPLE. International Archives of the Photogrammetry, Remote Sensing and Spatial Information Sciences - ISPRS Archives, 0, XLII-3/W10, 871-874.	0.2	0
270	DENOISING OF LIDAR ECHO SIGNAL BASED ON WAVELET ADAPTIVE THRESHOLD METHOD. International Archives of the Photogrammetry, Remote Sensing and Spatial Information Sciences - ISPRS Archives, 0, XLII-3/W10, 215-220.	0.2	5

#	Article	IF	CITATIONS
271	STUDY AND ANALYSIS OF REMOTE SENSING DATA PARALLEL PROCESSING. International Archives of the Photogrammetry, Remote Sensing and Spatial Information Sciences - ISPRS Archives, 0, XLII-3/W10, 443-450.	0.2	0
272	RESEARCH ON 3D BUILDING VISUALIZATION BASED ON TEXTURE SIMPLIFICATION AND FRACTAL COMPRESSION. International Archives of the Photogrammetry, Remote Sensing and Spatial Information Sciences - ISPRS Archives, 0, XLII-3/W10, 179-185.	0.2	0
273	OVERVIEW OF CHINESE AND AMERICAN MARINE AIRBORNE LIDAR. International Archives of the Photogrammetry, Remote Sensing and Spatial Information Sciences - ISPRS Archives, 0, XLII-3/W10, 111-115.	0.2	1
274	RESEARCH ON THE POLICIES AND LAWS OF INTERNATIONAL CIVILIAN REMOTE SENSING SATELLITES AND THEIR PROBLEMS. International Archives of the Photogrammetry, Remote Sensing and Spatial Information Sciences - ISPRS Archives, 0, XLII-3/W10, 821-824.	0.2	0
275	EXTRACTION OF HOUSES FROM POINT CLOUD LIDAR: PROBLEMS AND CHALLENGE. International Archives of the Photogrammetry, Remote Sensing and Spatial Information Sciences - ISPRS Archives, 0, XLII-3/W10, 831-837.	0.2	0
276	ORTHOPHOTO SHADOW DETECTION METHOD UNDER ARTIFICIAL SHADOW. International Archives of the Photogrammetry, Remote Sensing and Spatial Information Sciences - ISPRS Archives, 0, XLII-3/W10, 199-204.	0.2	0
277	DESIGN AND IMPLEMENT OF A CONICAL AIRBORNE LIDAR SCANNING SYSTEM. International Archives of the Photogrammetry, Remote Sensing and Spatial Information Sciences - ISPRS Archives, 0, XLII-3/W10, 1247-1252.	0.2	1
278	BLOCK ORTHORECTIFICATION AND MOSAIC OF 1960s DISP IMAGES IN QUJING, YUNNAN. International Archives of the Photogrammetry, Remote Sensing and Spatial Information Sciences - ISPRS Archives, 0, XLII-3/W10, 635-639.	0.2	0
279	FPGA-BASED ON-BOARD CUBIC CONVOLUTION INTERPOLATION FOR SPACEBORNE GEOREFERENCING. International Archives of the Photogrammetry, Remote Sensing and Spatial Information Sciences - ISPRS Archives, 0, XLII-3/W10, 349-356.	0.2	3
280	BASED ON GPU FOR STRIP ADJUSTMENT ALGORITHM OF LIDAR DATA. International Archives of the Photogrammetry, Remote Sensing and Spatial Information Sciences - ISPRS Archives, 0, XLII-3/W10, 229-233.	0.2	0
281	HOLE-FILLING ALGORITHM FOR AIRBORNE LIDAR POINT CLOUD DATA. International Archives of the Photogrammetry, Remote Sensing and Spatial Information Sciences - ISPRS Archives, 0, XLII-3/W10, 739-745.	0.2	2
282	CANOPY LIDAR POINT CLOUD DATA K-MEANS CLUSTERING WATERSHED SEGMENTATION METHOD. ISPRS Annals of the Photogrammetry, Remote Sensing and Spatial Information Sciences, 0, VI-3/W1-2020, 67-73.	0.0	2